Anti-HIV-1 activity of quinic acid isolated from *Helichrysum mimetes* using NMR-based metabolomics and computational analysis

Simin Emamzadeh Yazdi[a], Gerhard Prinsloo[b], Heino Martin Heyman[ac], Carel Basson Oosthuizen[a], Thomas Klimkait[d], Jacobus Johannes Marion Meyer[a*]

[a] *Department of Plant and Soil Sciences, University of Pretoria, Pretoria, Gauteng 0002, South Africa*

[b] *Department of Agriculture and Animal health, Florida Campus, University of South Africa (UNISA) 1710*

[c] *Bruker Daltonics Inc., Billerica, MA 01821, USA*

[d] *Molecular Virology, Department of Biomedicine, University of Basel, Basel, Switzerland*

[*] **Correspondence**

Marion Meyer, Department of Plant and Soil Sciences, University of Pretoria, Pretoria, South Africa 0002. Tel.: ++27-12-4202224; E-mail: marion.meyer@up.ac.za

Highlights

- NMR-based metabolomic analysis and determination of anti-HIV-1 activity of 32 South African *Helichrysum* species.
- The first report of the isolation of quinic acid from *H. mimetes* and its anti-RT activity.
- Molecular docking studies showed successful binding within the active site of RT and predicted the binding mode of quinic acid.

Abstract

Helichrysum species are widely used in traditional medicine with potential against infectious diseases. Extraction of the aerial parts of 32 *Helichrysum* species was done using polar (methanol:water (1:1)) and non-polar (hexane, dichloromethane and acetone) solvent systems. Anti-human immunodeficiency virus (HIV) bioassays revealed that polar extracts of *H. mimetes* and *H. chrysargyrum* (2.5 µg/mL), polar and non-polar extracts of *H. cephaloideum* (25 µg/mL) and polar and non-polar extracts of *H. zeyheri*, *H. setosum*, *H. platypterum* and *H. kraussii* at (2.5 µg/mL), had greater than 90% inhibitory activity. The polar extract of *H. mimetes* (100 µg/mL) exhibited 55.93 % reverse transcriptase (RT) inhibition as a possible indication of the mechanism of action. Proton NMR spectra of the polar extracts exhibited the presence of aromatic compounds and carbohydrate moieties. Principal component analysis (PCA) of the polar extracts showed clustering related to the activity of the extracts with good predictability scores ($Q^2 > 0.5$). However, orthogonal projections to latent structures discriminant analysis (OPLS-DA) predictability of the model was low based on the Q^2 at approximately 0.25. Quinic acid (QA) isolated from *H. mimetes* showed promising anti-RT activity (IC_{50} = 53.82 µg/mL) comparable to the positive drug control, doxorubicin (IC_{50} = 40.31 µg/mL). A molecular docking study revealed the probable binding site and conformation of QA within cavity 4, with a docking score of -8.03. The docking score of doxorubicin within cavity 4 was -7.87. These are the first reports of QA's HIV-1-RT activity, as well as doxorubicin's docking characteristics on this enzyme.

Keywords: Anti-RT, HIV-1, *Helichrysum,* Metabolomics, Molecular docking, Quinic acid

1. Introduction

The history of using natural products from medicinal plants as therapeutic agents is as ancient as human civilisation (Mukhtar et al., 2008). In conventional Western medicine, 50–60% of pharmaceutical commodities contain natural products or are synthetically derived from natural products and 10 to 25% of the commonly used prescribed medicines contain compounds isolated from plants (Cameron et al., 2005).

The *Helichrysum* genus belongs to the Asteraceae family and contains approximately 500-600 species occurring worldwide, displaying attractive flowers. There are about 244-250 species distributed in South Africa and Namibia. These species exhibit magnificent morphological diversity, which are subdivide into 30 groups. These species vary in shape and size and they are often fragrant (Lourens et al., 2008). Species of *Helichrysum* are used in the treatment of various medical conditions. The first written reports of the medicinal use of *Helichrysum* species dates back to 1727 when Boerhaave used it to treat anxiety and hysteria (Scott and Hewett, 2008). *Helichrysum* species are traditionally used in the treatment of wounds, infections and respiratory conditions. The extracts and essential oils of *Helichrysum* species have demonstrated promising biological activities such as: anti-oxidant, antimicrobial and anti-inflammatory activity (Lourens et al., 2004). Almost every morphological group of *Helichrysum* species has medicinal properties, and the broad spectrum of uses is not limited to a specific morphological group (Lourens et al., 2008). According to Appendino *et al*. (2007) an acetone extract of *H. italicum* yielded arzanol (a phloroglucinol α-pyrone), which inhibited HIV-1 replication in T cells and triggered the release of pro-inflammatory cytokines in LPS-stimulated primary monocytes (Appendino et al., 2007). An aqueous extract from *H. aureonitens* and its isolated compound, galangin, exhibited *in vitro* antiviral activity against Herpes simplex virus type I (HSV-1) at a concentration of 1.35 mg/mL and 6 µg/mL respectively

(Meyer et al., 1997, 1996). According to Lall *et al*. (2006) a combination of the two isolated prenylated chalcones and a pyranochalcone, isolated from *H. melanacme,* exhibited promising results against Influenza A virus (IC_{50}=0.01 mg/mL) (Lall et al., 2006). The chemistry of this genus is complex with a wide variety of chemical classes, among which acylphloroglucinols are common, often with prenyl or geranyl side chains. Dihydrochalcones and puranochalcones are also found in this genus. Phloroglucinols, excluding those belonging to the flavonoids, is a major class of compounds in some specific groups of *Helichrysum*. Isolation of diterpenes and triterpenes like squalene compounds are common from this genus (Lourens et al., 2008).

HIV infects vital cells of the human immune system, specifically $CD4^+$ T cells and dendritic cells. Two different types of HIV have been identified: HIV-1 and HIV-2 that differ in their *in vivo* virulence. HIV-2 is less pathogenic and mostly restricted to west Africa, whereas HIV-1 has various strains, which are further classified into groups and subgroups (Cohen et al., 2008). There are three key enzymes, which represent essential function in the HIV life cycle, namely reverse transcriptase (RT), integrase (IN), and protease (PR). *Helichrysum populifolium* showed inhibitory effects (63.78%) against the HIV-1 RT enzyme at 200 µg/mL (Heyman et al., 2009). Ethanol extracts of *H. aggregatum*, *H. filicaule* and *H. parvifolium* showed inhibitory effects on HIV protease at a concentration of 50 µg/mL (Filho et al., 2010). HIV-1-RT has a significant role in the initial stages of HIV replication: The transformation of single-stranded viral RNA into double-stranded DNA is a crucial step during HIV replication, a step catalyzed by RT (Priya et al., 2015).

HIV/AIDS has the potential to negatively impact the socio-economic development of societies because of the associated high adult mortality rate in some countries, especially in sub-Saharan Africa. Despite the development and progress made in general health care in response to HIV/AIDS in the 21st century, the HIV pandemic remains one of the most serious challenges to global health,

and probably will continue to be one of the leading causes of death and disability in the world for the coming decades. Since the initial description of HIV as the causative agent of AIDS, more than 60 million people have been infected with the virus, and more than 25 million people have died (Cohen et al., 2008).

Due to the synergistic relationship between medicinal chemistry, biological activity, bio-information and molecular simulation, the use of a variety of computational techniques such as molecular docking has increased during the last decade (Okada et al., 2010; Ramirez, 2016). Metabolomics is a well-known biological research technique used for the identification and quantification of metabolites in living systems (Schripsema, 2010), and is becoming an increasingly powerful tool for research on secondary metabolite discovery and production (Breitling et al., 2013). The goal of plant metabolomics is to identify all metabolites in a plant, both quantitatively and qualitatively. Due to the large number and the chemically complex composition of plant metabolites as well as their different characteristics, the detection of all metabolites in a given plant species still seems impossible. Yet, metabolite profiling can be used in conjunction with statistics (metabolomics) for the identification of the most important compounds present in plants (Schauer and Fernie, 2006). This technique is fast becoming a 'hotspot' in global biological research. With the development of NMR techniques and multivariate data analysis, metabolomics is playing an increasingly important role in every aspect of the biomedical and phytochemical research fields, including biomarker screening, quality control, activity and toxicity prediction, clinical chemistry, chemotaxonomy and environmental metabolism (Heyman et al., 2015; Liu et al., 2010). In metabolomical analyses, principal component analysis (PCA) involves a mathematical procedure that transforms a number of possibly correlated variables to a smaller number of uncorrelated variables called principal components. With the use of this procedure, a large number of complex

data sets can be reduced to less complex dimensionless datasets, which are easier to interpret (Liu et al., 2010). The orthogonal projections to latent structures (OPLS) analysis algorithm integrates an orthogonal signal correction filter to distinguish the variations in the data that are useful for the prediction of a quantitative response from the variations that are orthogonal to the prediction (Boccard and Rutledge, 2013).

The objective of molecular docking is to predict the best conformations of a ligand by using a score function in a conformational area which is established by the molecular target-binding site. It is also used to identify novel, potent ligands and as a predictive tool for binding. Molecular docking is able to explain the molecular mechanisms of action of the active molecules with a particular 3D conformation on different types of enzyme systems, such as RT (Ramirez, 2016).

Considering the large diversity of secondary metabolites and their remarkable therapeutic potential, new technologies and tools need to be developed and applied to improve rapid screening and isolation of bioactive natural components. Despite extensive investigation on *Helichrysum* species, the biological activity and/or chemical composition of many species still remain unidentified. The main objective of the present study was to investigate the anti-HIV and anti-RT activity of selected *Helichrysum* species using NMR-based metabolomics in order to reduce the time and costs for the isolation and identification of active principles by conventional methods.

2. Materials and methods

2.1 Plant material

The aerial parts of 32 *Helichrysum* species were collected from different geographical regions in South Africa during spring and summer of 2014 and 2015. The samples were obtained from

Kirstenbosch Botanical Garden (Cape Town, Western Cape), Voortrekker Monument Nature Reserve (Pretoria, Gauteng), Buffelskloof Nature Reserve (Mpumalanga) and Amsterdam (Mpumalanga). Plant species were identified by Dr M. Koekemoer and Ms J.A. Reddy from the South African National Biodiversity Institute (SANBI) and Mrs E.P. Van Wyk and Ms M. Nel from the H.G.W.J. Schweickerdt Herbarium. A representative of each species was collected and herbarium voucher specimens were deposited in the H.G.W.J. Schweickerdt Herbarium (PRU) of the University of Pretoria, South Africa (Table 1).

Table 1

Collected *Helichrysum* species and morphological groups (Hillard, 1983).

***Helichrysum* species**	**PRU[a] Voucher no.**	**Morphological group**
H. acutatum DC.	121012	21
H. adenocarpum D.C.	120986	28
H. albilanatum Hilliard	121022	30
H. argyrophyllum D.C.	120814	29
H. athrixiifolium (Kuntze) Moeser	121537	9
H. aureum (Houtt.) Merr.	121002	30
H. aureum (Houtt.) Merr. var. *monocephalum* (DC.) Hilliard	121008	30
H. caespititium (DC.) Harv.	121538	12
H. callicomum Harv.	121005	2
H. cephaloideum DC.	121018	24
H. chrysargyrum Moeser	121004	22
H. dasyanthum (Willd.) Sweet	120813	10
H. harveyanum Wild	121547	23
H. kraussii Sch. Bip.	121025	8
H. lepidissimum S. Moore	121009	19

H. mariepscopicum Hilliard	121013	29
H. milleri Hilliard	121015	30
H. mimetes S.Moore	121017	19
H. mundtii Harv.	121014	23
H. mutabile Hilliard	121021	30
H. nudifolium (L.) Less. var. *nudifolium*	121003	23
H. opacum Klatt	121019	24
H. patulum (L.) D.Don	121536	18
H. petiolare Hilliard & B.L.Burtt	121535	18
H. platypterum DC.	121011	20
H. polycladum Klatt	121016	8
H. quinquenerve (Thunb.) Less.	121010	23
H. reflexum N.E.Br.	121006	29
H. setosum Harv.	121539	30
H. truncatum Burtt Davy	121020	13
H. wilmsii Moeser	121007	29
H. zeyheri Less.	121534	1

[a] H.G.W.J.Schweikerdt Herbarium of the University of Pretoria.

2.2 Preparation of extracts

Dried aerial parts of all 32 species (5 g) were ground to small pieces of approximately 0.4 mm. The following solvents (with increasing polarity); hexane, dichloromethane, acetone and methanol:water (1:1), were used for sequential extraction (Table 2). The extraction of the plant material was done in 40 mL steel pressure vessels with a SpeedExtractor E-914/E-916 from Buchi (Switzerland) using the parameters in Table 2. Thereafter, the filtrate was concentrated under vacuum to dryness using a Genevac (EZ-2 Plus, GeneVac, UK). The hexane, dichloromethane and acetone extractions were combined and is referred to as the non-polar extract, while the methanol:

water extract were kept separately as the polar extract. The samples were stored at 4°C and used for the anti-HIV bioassays, RT inhibition and NMR analysis.

Table 2

Extraction parameters for samples.

Parameter	Value/Solvent
Temperature	50°C
Pressure	100 bar
Solvents	Hexane, dichloromethane, acetone, methanol: water (1:1)
Cycles	2
Heat-up	1 min
Hold	15 min
Discharge	5 min
Flush with solvent	5 min
Flush with gas	8 min

2.3 Extraction of *H. mimetes* for the isolation of active compound(s)

For the isolation and purification processes, 30 g of air-dried aerial parts of *H. mimetes* was extracted with a SpeedExtractor as described above (Table 2). The extract was concentrated to dryness using a GeneVac as described above and resulted in 8.33 g of extract.

2.4 Isolation procedure and identification of isolated fractions/compounds

Five grams of the extract was subjected to fractionation on a silica gel 60 column (500 ml, 6.5 × 10 cm), using hexane-ethyl acetate, ethyl acetate-methanol and methanol:water mixtures of increasing polarity. From 16 collected fractions, fraction number 15 gave the best activity and low toxicity and was subjected to Sephadex LH-20 column using methanol as eluent to isolate the active compound(s).

To elucidate the possible presence of chlorogenic acid type compound(s) in the isolated fractions, the TLC plates (pre-coated Merck TLC plates with adsorbent silica gel 60 F254) were sprayed with the natural products reagent (NP/PEG) (Cretu et al., 2013). This was prepared and sprayed by dissolving 2 g of diphenylborinic acid aminoethylester (NP) and 10 g of polyethylene glycol 400 (PEG) separately in 200 mL of ethyl acetate. The TLC plate was then viewed under UV light at $\lambda = 366$ nm.

2.5 Bioassays

2.5.1 Anti-HIV screening assay

All non-polar and polar extracts (64 in total) were screened in duplicate for anti-HIV activity using a colorimetric cell-based (HeLa-SXR5) assay at 2.5 µg/mL and 25 µm/mL concentrations as described previously (Heyman et al., 2015). Extracts were prepared in cell culture medium with a final DMSO concentration of 5%. A positive drug control, Efavirens (a non-nucleotidic RT inhibitor, Sigma-Aldrich, St. Louis, USA) and negative control (PBS 5% DMSO) were included in the assay. The analysed inhibitory range in patients is comparable with the *in vitro* activity in this replicative system (Heyman et al., 2015). The bioassay produces replication in a time window of 4 days (deCIPhR) as previously described (Vidal et al., 2012). To investigate the toxicity of the plant extracts, cytotoxicity and cell morphology of the culture were investigated microscopically after 4 days.

The isolated fractions of the most active extract were also tested against replicative HI viruses as described above to determine the most active fraction(s).

2.5.2 HIV-1 reverse transcriptase colorimetric assay

Enzymatic RT inhibition of the active extracts was evaluated using a non-radioactive HIV-RT colorimetric ELISA kit (Roche, Germany) according to the method described by Fonteh *et al*. (Fonteh et al., 2009). The extracts were tested at 50 µg/mL and 25 µg/mL. The recombinant HIV-1 RT (0.2 U) and extract were incubated for 1 h at 37°C. Subsequently, an antibody conjugated to peroxidase was added that binds to the digoxigenin–labeled DNA. In the final step, the 2.2`-azino-bis-(3-ethylbenzothiazoline-6-sulfonic acid) (ABTS substrate solution) is cleaved by the peroxidase enzyme, producing a colored reaction product. Doxorubicin, an anticancer drug and also an inhibitor of viral RT was employed as a positive drug control at 50 µg/mL and 25 µg/mL. The experiment was conducted in duplicate. The absorbance values of the samples were measured at 405 nm with a reference wavelength set at 492 nm using a microtiter plate reader (Multiskan Ascent; Thermo Labsystems; USA).

2.6 NMR based metabolomic analysis of polar extracts and isolated fractions

The polar extracts and fractions were re-dissolved to a concentration of 15 mg/mL in a buffered mixture of CD_3OD (Sigma, USA) and a KH_2PO_4 (Fluka, Germany)-D_2O (Sigma, USA) solution, with the pH adjusted to pH 6 with NaOD (1.0 M) (Sigma, USA). Trimethylsilane propionic acid sodium salt (0.1 % TSP – 0.00 ppm) was used as internal standard for spectral referencing of the polar samples.

Polar samples and fractions (800 µL) were transferred to 5 mm NMR tubes and 128 scans were recorded with a spectral width of 14 ppm on a Varian 600 MHz spectrometer (proton frequency 600.13 MHz). Temperature was kept constant at 25 °C. The ^{1}H NMR spectra were reduced to ASCII files using MestReNova 10.0 (Mestrelab Research, Spain). All ^{1}H NMR spectra were referenced to the internal TSP standard, phased, baseline corrected and normalized. The spectra

were then reduced to bins of 0.04 ppm in width to generate a set of integrated bins. This 'binned' data was exported to Excel (Microsoft, USA) and analysed using SIMCA-P 13.0.0 (Umetrics, Umeå, Sweden) statistical analysis software. The region ranging from 3.28 - 3.36 ppm (residual MeOH) and 4.60 - 5.00 ppm (residual water) were removed prior to statistical analyses of the polar samples. The data was Pareto scaled before PCA and OPLS analyses. The spectral data of the fractions was compared to the contribution plot by comparing the values of the specific buckets to the importance coefficient of the extract/fraction and activity profile.

2.7 Molecular docking of quinic acid

The 3D crystal structure of the target; HIV-1 RT (PDB ID: 1RTH) was retrieved from the protein data bank and prepared using the protein preparation wizard in Maestro (Schrödinger suite v2017). Briefly, the structure was observed and preprocessed by the addition of hydrogens, bond order assignments and the removal of all crystallographic water molecules from the structure. Hydrogen bonds were optimized and the protonation states were predicted using PROPKA at a pH of 7.0 and finally, the enzyme undergone a restrained, minimized using the OPLS3 force field (Harder et al., 2015). The active isolated compound from *H. mimetes*, quinic acid (QA) and the enzyme assay positive control (doxorubicin) was drawn on UCSF Chimera and imported into Maestro (Meng et al., 2006). These two compounds together with the reference ligand U05 (co-crystal inhibition, a nevirapine derivative) were prepared and minimized using LigPrep (Fig. 1). Epik was used to generate possible states at a pH of 7.0 and the OPLS3 force field was used for energy minimization.

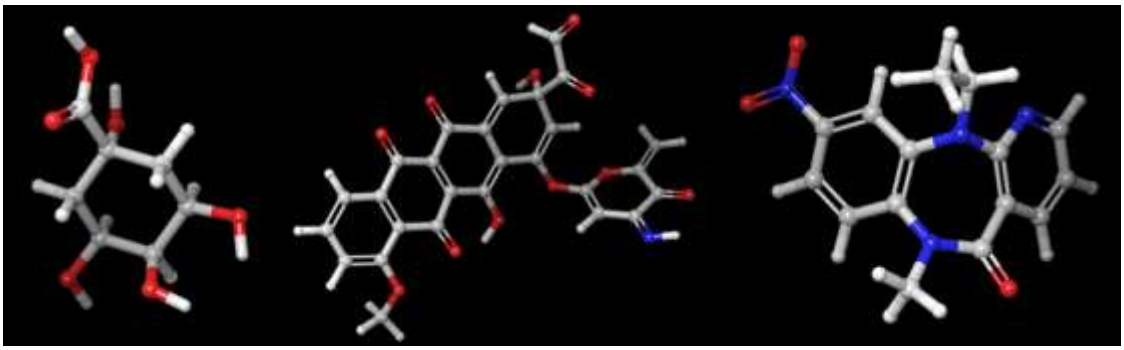

Quinic acid Doxorubicin Reference ligand, U05

Fig. 1. Three-dimensional structures of minimized ligands used in the docking study.

The catalytic residue of protein 1RTH was examined using SiteMap (Schrödinger, LLC 2018, USA) by a simple Van der Waals probe and the interaction energy to locate energetically favourable binding sites (Halgren, 2007, 2009). The five most favourable binding sites or cavities were identified. Receptor grid files were prepared for each identified site using the receptor grid generation tool at a 6A region around the centre. A flexible docking was performed with the potential active sites detected on HIV-1-RT enzyme using Glide software. Docking of the 3D structures of QA, doxorubicin and U05 in the active sites were performed using the extra-precision (XP) function. All molecules were evaluated for possible molecular interactions with active site residues using the pose viewer visualizer (Friesner et al., 2006; Halgren et al., 2004).

2.8 Statistical analysis

All data were analysed statistically and the IC_{50} values of each extract were obtained using GraphPad Prism (GraphPad Software Inc., USA) by using a 4-parameter logarithmic equation with constraints on the top (100) and bottom (0) parameters. Data for RT inhibition were analysed for statistical significance and expressed as mean values ± standard deviation (SD) where $p < 0.05$ were considered statistically significant.

3. Results and discussion

3.1 Anti-HIV screening assay

The results of the screening activity against HIV are given in Table 3. Several polar extracts (*H. albilanatum, H. mimetes*, *H. platypterum*, *H. patulum*, *H. mutabile*, *H. dasyanthum*, *H. lepidicimum*, *H. harveyanum*, *H. chrysargyrum*, *H. opacum*, *H. aureum*, *H. truncatum*, *H. kraussii*, *H. nudifolium*, *H. setosum, H. wilmsii* and *H. zeyheri*) exhibited promising HIV inhibition at 2.5 µg/mL (>80%) and only *H. acutatum* showed cytotoxicity. Nine polar extracts (*H. adenocarpum*, *H. aureum var monocephalum*, *H. caespititium*, *H. cephaloideum, H. chrysargyrum*, *H. mareipscopicum*, *H. millerii*, *H. mimetes* and *H. quinquenerve*) showed significant inhibition against HIV at the higher concentration (25 µg/mL) while the rest displayed cytotoxicity activity. The non-polar extracts of *H. callicomum*, *H. cephaloideum*, *H. kraussii*, *H. millerii*, *H. platyptrum*, *H. polycladum*, *H. setosum* and *H. zeyheri* showed anti-HIV activity (≥ 85%) at 25 µg/mL and the remaining extracts showed cytotoxicity at this concentration. The non-polar extracts had no inhibition nor cytotoxicity at 2.5 µg/mL against the HI virus (Table 3). Among all extracts with activity, the best results were obtained with the polar extracts of *H. mimetes* and *H. chrysargyrum* at 2.5 µg/mL and 25 µg/mL, polar and non-polar extracts of *H. cephaloideum* at 25 µg/mL, polar and non-polar extracts of *H. zeyheri*, *H. setosum*, *H. platypterum* and *H. kraussii* at 2.5 and 25 µg/mL, all with higher than 90% inhibitory activity.

The cytotoxicity findings of some *Helichrysum* species analysed in this study are supported by Lourens *et al*. (Lourens et al., 2011). They tested the *in vitro* cytotoxicity of 35 indigenous South African *Helichrysum* species and found that *H. aureum* var. *aureum* and *H. platypterum* had less than 10% cytotoxicity on transformed human kidney epithelial (Graham) cell growth at 0.1 mg/mL (Lourens et al., 2011). Lourens et al. also observed more than 80% growth for the 'normal' Graham

cells with extracts of *H. adenocarpum*, *H. appendiculatum*, *H. cephaloideum* and *H. indicum*, while the growth of the breast cancer cell line MCF-7 was reduced by more than 50% at the same concentration of the extract, indicating a certain cell-type selectivity. *H. petiolare* showed minimal growth inhibition at 0.1 mg/mL (Lourens et al., 2011). Although *Helichrysum* species are generally not toxic to humans, preliminary results of the current study suggest that the use of toxicity studies are necessary when organic solvents such as dichloromethane and methanol are used for extract preparation.

Table 3

Anti-HIV screening result (% inhibition) of *Helichrysum* species. No activity against HIV was observed for any of the non-polar extracts at 2.5 µg/mL.

Plant species	**% Inhibition**		
	25 µg/mL Polar	2.5 µg/mL Polar	25 µg/mL Non-polar
H. acutatum	CA	CA	CA
H. adenocarpum	122	ND	ND
H. albilanatum	CA	85	CA
H. argyrophyllum	CA	ND	CA
H. athrixifolium	CA	NA	CA
H. aureum var *aureum*	CA	95	CA
H. aureum var *monocephalum*	126	ND	CA
H. caespititium	124	ND	CA
H. callicomum	CA	ND	108
H. cephaliodeum	115	ND	108
H. chrysargyrum	120	103	CA
H. dasynthum	CA	110	CA
H. harveyanum	CA	107	CA

H. kraussii	CA	97	125
H. lepidisimum	CA	108	CA
H. mariepscopicum	121	ND	CA
H. millerii	133	ND	129
H. mimetes	132	121	CA
H. mundtii	CA	ND	CA
H. mutabile	CA	111	CA
H. nudifolium var. *nudifolium*	CA	92	ND
H. opacum	CA	100	CA
H. patulum	CA	114	CA
H. petiolare	CA	ND	CA
H. platypterum	CA	118	100
H. polycladum	CA	ND	95
H. quinquenerve	120	ND	CA
H. reflexum	CA	ND	CA
H. setosum	CA	81	103
H. truncatum	CA	98	CA
H. wilmssii	CA	118	CA
H. zeyheri	CA	105	85

CA: Cytotoxic Activity observed, NA: No Activity.

3.2 HIV-1 reverse transcriptase colorimetric assay

The inhibitory potential of all active extracts in the live anti-HIV bioassay was determined on the RT enzyme tested to determine the probable mechanism of action. The results showed that five of these polar extracts had more than 50% HIV-1 RT inhibition at a concentration of 100 µg/mL (Table 4), whereas the other *Helichrysum* species extracts (polar and non-polar) did not exhibit any inhibition on the RT enzyme. Doxorubicin displayed inhibitory activity with an IC_{50} value of 23.55

µg/mL. In a study conducted by Min *et al*. (Min et al., 2000), doxorubicin was used as a positive control, which inhibited RT activity with an IC_{50} value of 25.001 µg/mL. This result on doxorubicin has also been supported in a study by Kapewangolo *et al*.(Kapewangolo et al., 2013).

Table 4

Anti-HIV-RT inhibition of anti-HIV active polar extracts at 100 µg/mL.

***Helichrysum* species**	**RT % Inhibition ± SD**
H. platypterum	61.01 (±7.4)
H. mariepscopicum	59.55 (±7.7)
H. mimetes	55.93 (±2.1)
H. cephaloideum	55.32 (±3.3)
H. caespititium	52.79 (±4.8)
Doxorubicin (50 µg/ml)	94.31 (±2.6)

There are limited reports on the inhibition of the HIV-1 RT by *Helichrysum* species. A study by Heyman *et al.* (2009) revealed that *H. populifolium* had a significant inhibitory effect for the HI virus and showed inhibitory activity against HIV-RT at 200 µg/mL (Heyman et al., 2009).

3.3 NMR-based metabolomic analysis of polar extracts

All polar extracts were subjected to metabolomic analysis. In order to fast-track the selection of the best extract for active compound purification, metabolomic tools were used to aid it by investigating differences in the chemical profiles of the extracts of the 32 *Helichrysum* species using ^{1}H NMR spectroscopy. The NMR spectra of the polar extracts especially showed the presence of aromatic compounds (6.00 - 8.00 ppm) and carbohydrate moieties (3.00 - 6.00 ppm). PCA was used to determine if the *Helichrysum* species with anti-HIV activity had similar compounds, which are not present in the non-active species. Since all samples belonged to the *Helichrysum* genus, it was

predicted that not many different groups would be obtained in the PCA. The datasets used for the PCA score plots did not show distinct grouping correlating with the activity of the extracts but PC5, PC4 and PC2 demonstrated a separation of *H. mimetes* and *H. lepidissimum* from the rest of the species. The PC5 result was similar as PC2 and PC4 but *H. opacum* was observed as an outlier. This indicates that there is a marked phytochemical difference between this group and the rest of the samples. The PCA model with $R^2X = 0.80$ and $Q^2 = 0.61$ values for component 5 indicated good predictability and reliability of the model (Fig. 2).

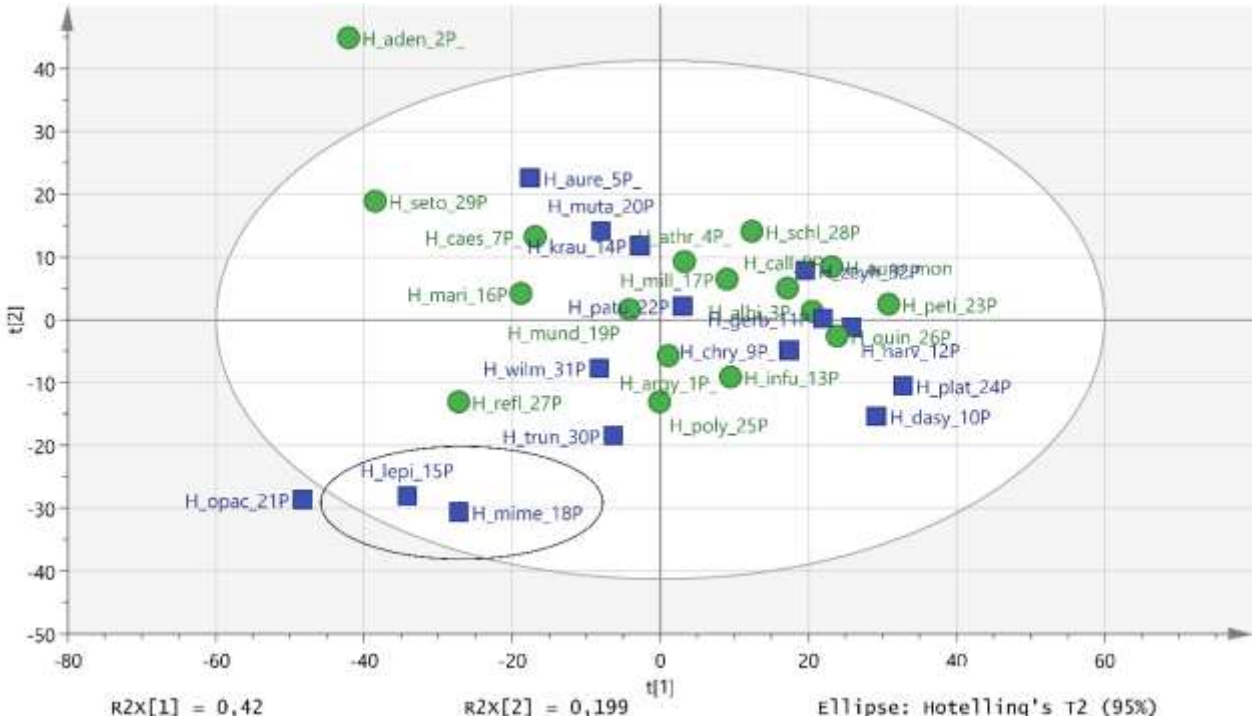

Fig. 2. PCA score plot did not exhibit significant correlation between active and non-active *Helichrysum* polar extracts. R^2X: 0.80 and Q^2 (cum): 0.61. ■ Active extracts, ● Extracts with no activity. *H. mimetes* and *H. lepidissimum* clustered closely together in all PC`s.

In the OPLS-DA analysis, anti-HIV activity data was included as a secondary observation, which assisted in the correlation of the phytochemical composition and biological activity of the samples. The extent of grouping on similarity in chemical composition and bioactivity was good in this analysis (Fig. 3). It explained the differences between the two groups on HIV activity quite

well as indicated by the good $R^2Y = 1.00$ value. The active *H. mimetes* and *H. lepidissimum* polar extracts clustered closely together and are well separated from the rest of the polar extracts (Fig. 3). It indicates that, based on biological activity; there is a distinct phytochemical difference between these two extracts and the rest of the samples. The variation in X explains as much of the variation with the R^2X (cumulative) being 75%. The predictive component (P1) only explained 4.6% of the variation in X related to the separation of the samples based on the activity. Based on the Q^2 of approximately 0.25, the predictability of the model was not significant. The obtained result was comparable to that of a study on other *Helichrysum* species by Heyman *et al.* (they reported a Q^2 value of 0.3) (Heyman et al., 2013). However, the achieved R^2 value of the current study showed better fitness of the model.

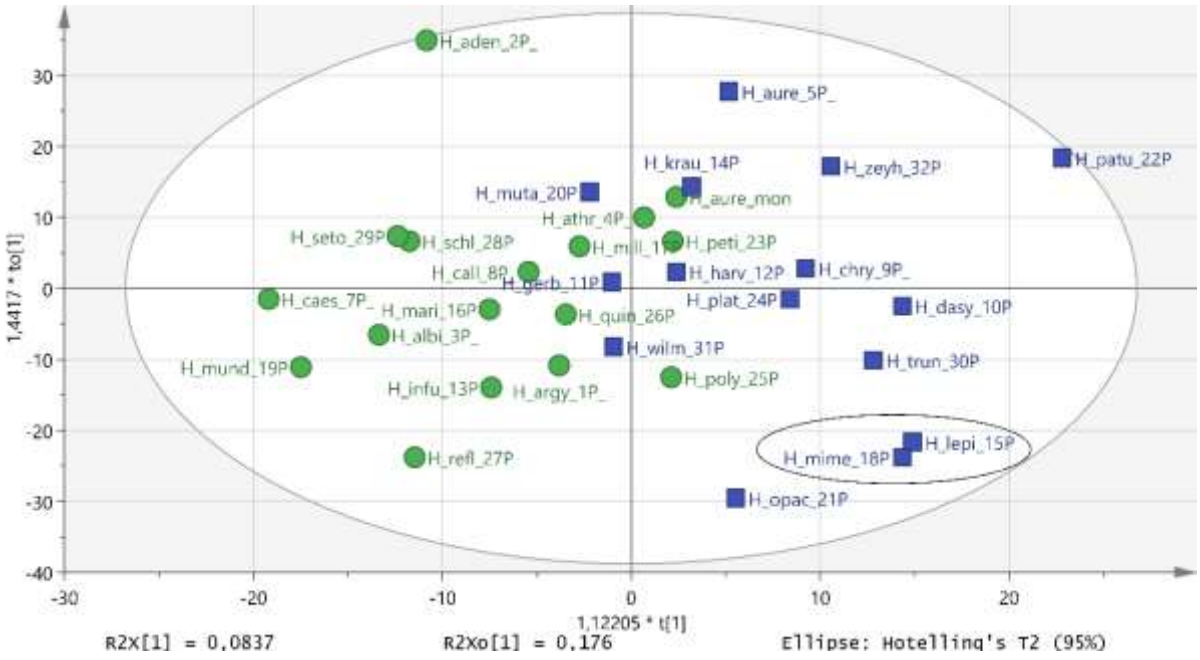

Fig. 3. The OPLS-DA score plot exhibit significant correlation between *Helichrysum* polar extracts. ■ Active extracts, ● Extracts with no activity. *H. mimetes* and *H. lepidissimum* polar extracts clustered closely together.

3.4 Anti-HIV and anti-RT activity of isolated *H. mimetes* fractions

Based on the activity and metabolomic results of the 32 species selected for this study, *H. mimetes* was subjected to isolation and identification of active compounds. All 16 isolated fractions and *H. mimetes* crude extract were tested in a live HI virus assay at two concentrations (2.5 µg/mL and 25 µg/mL) (Fig. 4). Fractions 1-5 showed no activity, whereas fractions 6-13 had anti-HIV activity but significant toxicity at the same concentrations. However, fractions 14 and 15 showed antiviral activity in the absence of toxicity. The crude extract illustrated very good inhibition with no cytotoxicity at the highest concentration (25 µg/mL), which probably reflected synergistic interactions of the chemical entities in the extract.

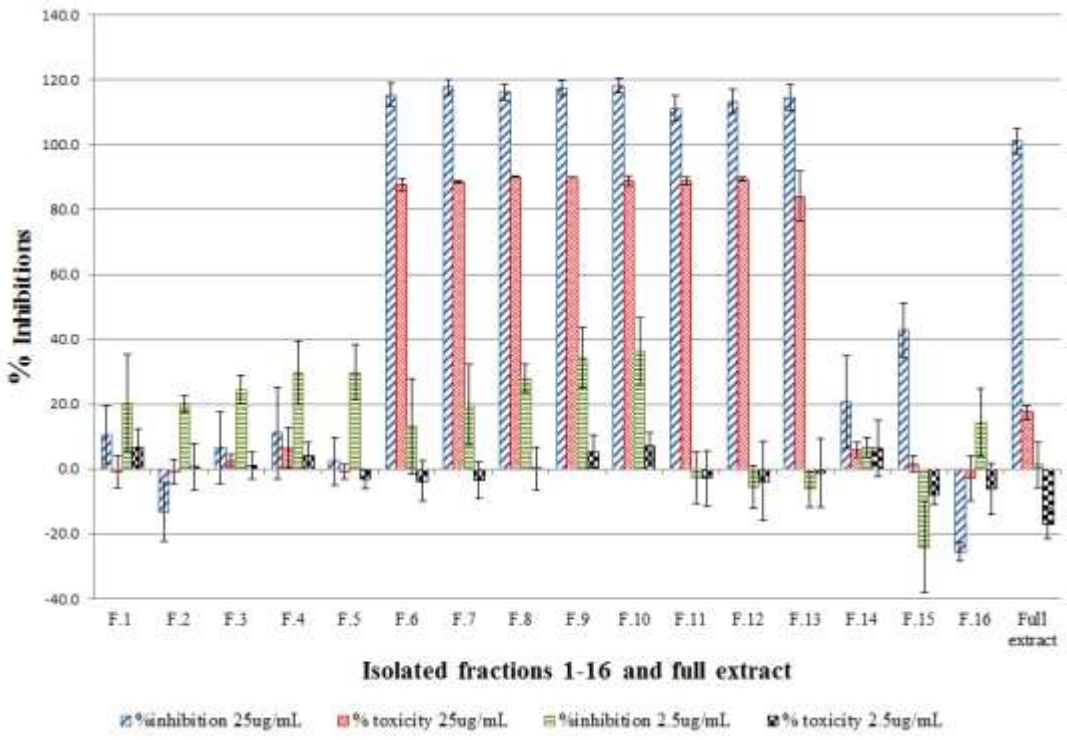

Fig. 4. Anti-HIV activity and toxicity of crude extract and 16 isolated fractions from *H. mimetes* against HI live virus at two concentrations (2.5 µg/mL and 25 µg/mL).

Isolated fractions were subjected to a RT inhibition screening assay at two concentrations (25 µg/mL and 50 µg/mL). The most significant results are represented in Table 5. Fraction 15 exhibited

a promising anti-RT result especially at the higher concentration (50 µg/mL). Therefore, fractions 14 and 15 were analysed at different concentrations against RT enzyme to calculate the IC_{50} values.

Table 5

The best results of the anti-RT inhibition assay of isolated fractions.

Fraction	**% RT inhibition ± SD**
F14 (50 µg/mL)	23.894 (± 5.550)
F15 (50 µg/mL)	65.618 (± 1.464)
F15 (25 µg/mL)	40.584 (± 0.183)

Fraction 15 exhibited promising activity in the anti-RT assay with an IC_{50} value of 54.82 µg/mL, which is comparable to that of doxorubicin which had an IC_{50} value of 40.31 µg/mL (Table 6 and Fig. 5).

Table 6

Anti-RT activity of fractions 14 & 15.

Fraction	IC_{50} (µg/mL) ± SD
F 14	199.3 (± 8.4)
F 15	54.82 (± 4.2)
Doxorubicin	40.31 (± 3.3)

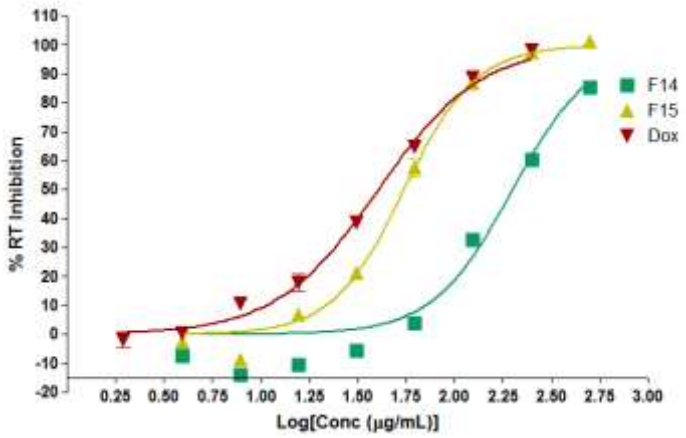

Fig. 5: Inhibition of HIV-RT by fractions F14 & F15 and doxorubicin at different concentrations.

3.5 NMR-based metabolomic analysis of *H. mimetes* fractions and identification of active compound

The ^{1}H NMR spectra of fractions 6–13 showed signals at chemical shifts that are most likely caffeoylquinic acids (Heyman et al., 2015). Chlorogenic acids, including caffeoylquinic acids, have often been identified in the extracts of *Helichrysum* species (Albayrak et al., 2010). The NMR chemical shifts associated with caffeoylquinic acids are 2.56-3.08 ppm, 5.24-6.28 ppm, 6.44-7.04 ppm and 7.24-8.04 ppm. The TLC analysis also supported this finding by showing the presence of compounds in these fractions with a light blue/green fluorescent colour under UV light at λ = 365 nm with visualization by the NP/PEG reagent (Cretu et al., 2013). There was however no such colour reaction in fractions 14 and 15 (Fig. 7). The anti-HIV activity of caffeoylquinic acids has previously been shown (Heyman et al., 2015) and thus probably explains the activity found in fractions 6-13.

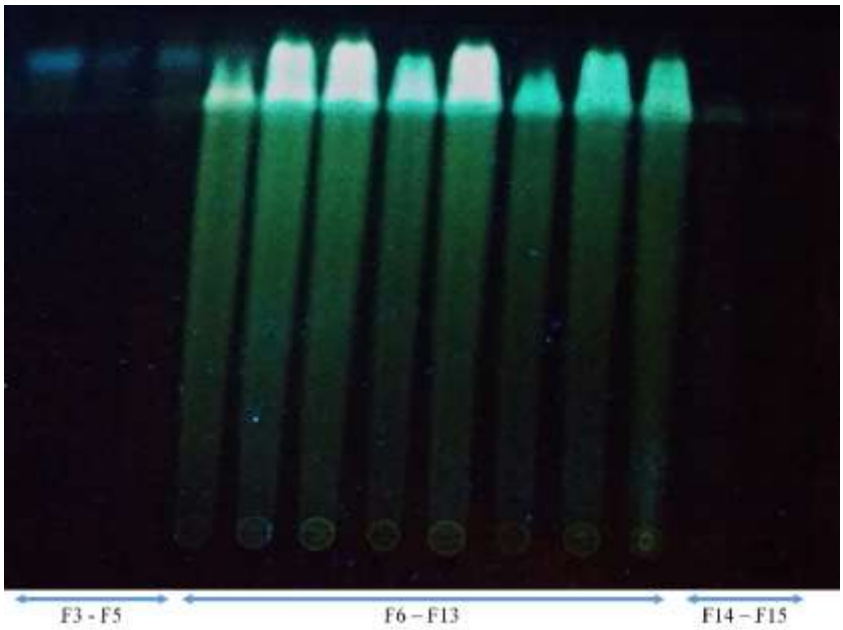

Fig. 7. Light blue/green fluorescence under UV light at λ = 365 nm with NP/PEG reagent indicated the presence of caffeoylquinic acids in fractions 6-13, but not in other fractions.

The ^{1}H NMR spectra of fractions 14 and 15 however showed that the active component could not be caffeoylquinic acids due to the absence of the related chlorogenic acids chemical shifts in these fractions. PCA and OPLS-DA were employed to differentiate the isolated fractions based on their chemical profiles. The results of the PCA showed good grouping based on the chemical shifts of the fractions with $R^2 = 0.953$ and $Q^2 = 0.778$ (Fig. 6). In the OPLS-DA the anti-RT activity data was included as a secondary observation. The active fraction 15 is separated from the rest of the fractions indicating a significant phytochemical difference with the others. Based on the Q^2 values in both PCA and OPLS-DA at 0.77 and 0.78, respectively, the predictability of the models was significant. It was therefore decided to purify fraction 15 by using a Sephadex LH-20 column. A ^{1}H NMR analysis of the isolated sub-fractions showed that the chemical shifts of the purified compound present in the fraction 15 and responsible for its anti-RT activity was quinic acid (QA). This was confirmed with comparison to an authentic standard sample of QA.

PCA OPLS-DA

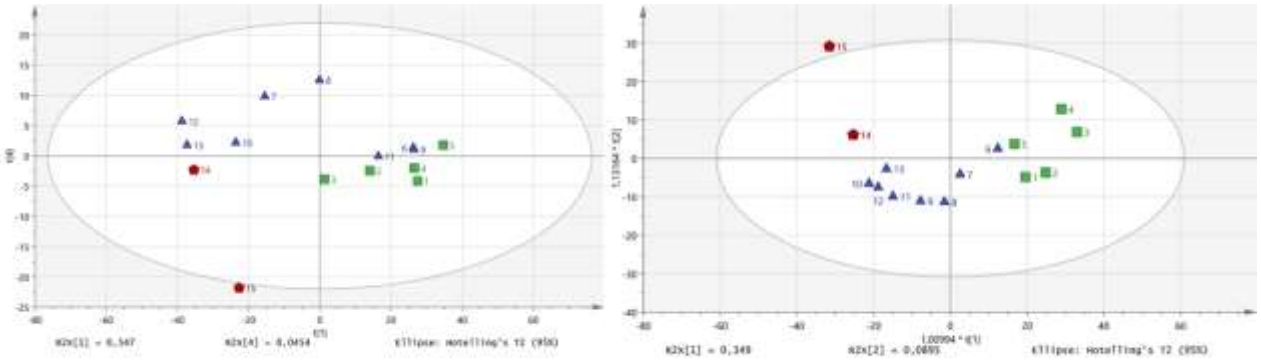

Fig. 6. PCA ($R^2 = 0.953$/ $Q^2 = 0.778$) & OPLS-DA ($R^2 = 0.892$/$Q^2 = 0.784$) score plots of isolated fractions. ■ Fractions 1-5, ▲ Fractions 6-13, ⬟ Fractions 14-15.

3.6 Molecular docking analysis

A total of five cavities or receptor sites were detected in the reverse transcriptase enzyme by using SiteMap and were named cav1, cav2, cav3, cav4 and cav5. The volume and surface area details are represented in Table 7.

The 3D structure of HIV-1-RT was analyzed, and QA was optimized to have minimal potential energy using Chimera. The catalytic site amino acid residues were identified for HIV-1-RT using SiteMap. Docking studies were performed on all sites. The catalytic site amino acids in domain A of HIV-1-RT are included in Table 7. This catalytic site residues were loaded as an input in Glide software as a receptor grid file, to eliminate other amino acid residues and select only catalytic site amino acids of the HIV-1-RT. Evaluation of the binding mode and its stability with QA to HIV-1-RT were performed using Glide.

Table 7

Possible binding sites and cavity prediction of HIV-RT (PDB: 1RTH)

Cavity	Volume (Å)	Size[a]	SiteScore[b]	Dscore[c]	Phobic[d]	Philic[e]	Residues[f]
Cav 1	1188.84	314	1.01	1.03	0.44	1.01	Chain B: 29,30,33,36,37,40,41,62,63,64,65,66,67,68,70,71,72,73,74,75,107,108,109,110,111,112,113,16,146,151,152,185,186,188,199,202,203,206,214,215,216,217,231,232,233,234,235,238,239,240,241,242,339,350,351,352,353,354,357,358,360,366,370,371,373,374,375,377,378,403,404,405,406,407,408,409,410,430,431,432,433
Cav 2	607.45	280	1.06	1.07	0.71	1.05	Chain A: 6,8,88,89,90,91,92,93,94,95,115,17,158,160,161,162,165,166,169,172,173,175,176,178,179,180,181,182,183,184; Chain B: 23,49,50,51,52,131,133,134,137,138,139,140,141,142,143
Cav 3	643.47	239	1.09	1.03	0.74	1.24	Chain A: 363,364,365,400,401,403,404,405,406,424,425,426,427,428,429,430,

Cavity	Volume (Å)	Size[a]	SiteScore[b]	Dscore[c]	Phobic[d]	Philic[e]	Residues[f]
							431,503,506,507,508,509,511,532, 533,534,535; Chain B: 247,249,252,255,256,258,259,260, 262,263,330,331,332,333,334,392, 419,421,422,424,425,428,429
Cav 4	394.45	194	1.15	1.20	2.13	0.73	Chain A: 95,99,100,101,102,103,106,172,17 9,180,181,182,188,189,190,227,22 9,234,235,236,318,319,382,383; Chain B: 28,31,32,35,134,135,136,138,139,1 40,142
Cav 5	419.83	119	1.06	1.09	0.44	0.92	Chain B: 74,75,76,77,78,81,82,86,87,93,94,1 52,154,157,158,182,183,184,185,3 24,325,385,386,387,388,409,410,4 11,412,413

[a]Size of the cavity given in number of site points, [b]SiteScore gives an overall quality of the binding site (SiteScore = 0.0733 sqrt(n) + 0.6688 e - 0.20 p), [c]druggability score, [d]score of hydrophobic characteristic, [e]score of hydrophilic characteristic, [f]domain and residue number involved in the cavity.

The binding conformations of QA to HIV-1-RT was determined, and the one having the lowest binding energy among the different conformations was generated. The result of this analysis

was compared to the protein reference (U05- nevirapine derivative) and doxorubicin (Table 8). The lower energy score or docking score represents a possible better prediction of protein-ligand binding affinity as opposed to higher energy values.

Table 8

Molecular docking results of quinic acid (QA), doxorubicin (Dox) and reference ligand U05 (Ref) within the five binding sites identified.

Cav	Compounds	R bonds	XP GScore	glide evdw	glide ecoul	glide energy	glide einternal	glide emodel	XP HBond
	Dox	7	-8.62	-54.35	-4.71	-59.06	5.61	-79.34	-1.46
1	QA	6	-7.87	-21.94	-9.65	-31.59	1.20	-36.50	-4.59
	Ref	2	-5.31	-35.85	-2.64	-38.49	0.38	-48.29	-0.22
	QA	6	-8.69	-27.48	-7.93	-35.41	3.24	-42.85	-4.67
2	Ref	2	-3.98	-25.17	0.23	-24.94	6.01	-18.85	-0.30
	QA	6	-7.55	-15.95	-17.09	-33.04	2.83	-42.40	-3.56
3	Dox	5	-4.32	-42.96	-5.23	-48.20	16.22	-39.80	-0.77
	Ref	2	-2.18	-29.49	-3.6	-33.11	1.10	-42.32	0
	Ref	2	-9.55	-47.13	-2.92	-50.05	0.07	-77.34	0
4	QA	6	-8.03	-22.50	-12.92	-35.42	2.29	-42.7	-3.97
	Dox	7	-7.87	-42.20	-10.51	-52.71	6.11	-48.04	-1.66
	QA	6	-6.88	-19.74	-13.91	-33.65	1.33	-39.89	-3.36
5	Dox	7	-6.18	-32.29	-8.69	-40.98	3.32	-59.98	-2.20
	Ref	2	-2.93	-28.14	-3.38	-31.52	0.94	-40.84	-0.91

The docking was performed successfully with all three ligands into the five cavity sites, except for doxorubicin, which did not dock into cavity 2. Among the ligand-receptors, the co-crystallized reference ligand, U05's crystal structure showed the lowest binding energy within cavity 4 (identical to the crystal structure), with a docking score of -9.55, this was followed by QA and

doxorubicin with docking scores of -8.03 and -7.87, respectively, in the same site (Figs. 8, 9, 10). QA had relatively low docking scores for two of the predicted binding sites, cavities 4 and 2, indicating a high affinity for these two sites. Figure 8 depicts the binding and conformation of QA and the reference ligand within cavity 4. Interestingly, the study revealed the probable binding site and conformation of doxorubicin within cavity 1, with a docking score of -8.62 and an emodel value of -79.34. The emodel value for the reference structure in cavity 4 was -77.34, indicating the high probability of doxorubicin binding in the identified site. The emodel value combines the docking score, the non-bonded interaction energy and the internal strain energy of the ligand conformation. Doxorubicin is structurally larger than the other two ligands and it performed the best in cavity 1 with the largest volume of 1188.84 Å (Fig. 10).

On analysis of the binding mode of QA into the catalytic site of HIV-1-RT (cavity 4) it was found that the residues Lys 101 and Tyr 188 were involved in the H-bond interaction. Moreover, they contributed three hydrogen bonds between them (Figure 8).

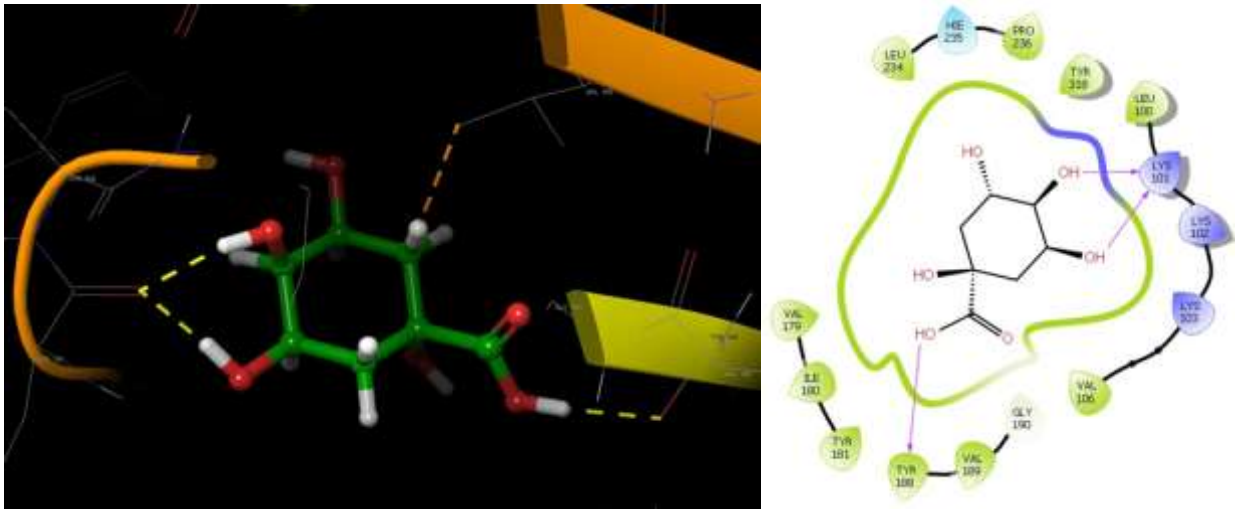

Fig. 8. Quinic acid docked in cavity 4 with a docking score -8.03 (left), interaction diagram of QA indicating the hydrogen bonds between the ligand and binding site residues A: Tyr 188 and A: Lys 101 (right).

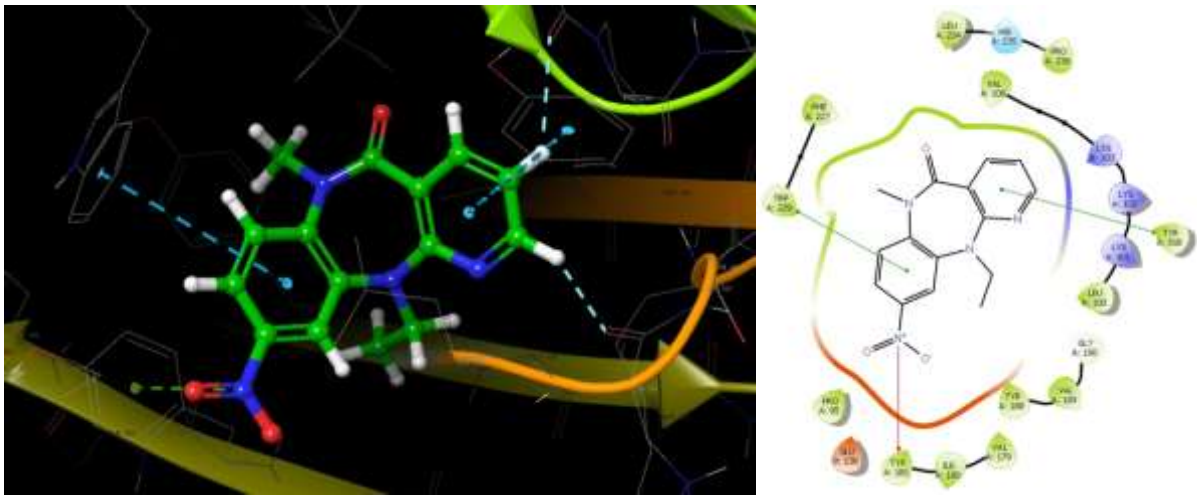

Fig. 9. Reference compound U05 docked in cavity 4 with a docking score of -9.55 (left), interaction diagram of the Reference ligand indicating the salt bridges between ligand and residue A: Tyr 181 and pi-pi stacking with residues A: Trp 229 and A: Tyr 318the ligand and binding site residues (right).

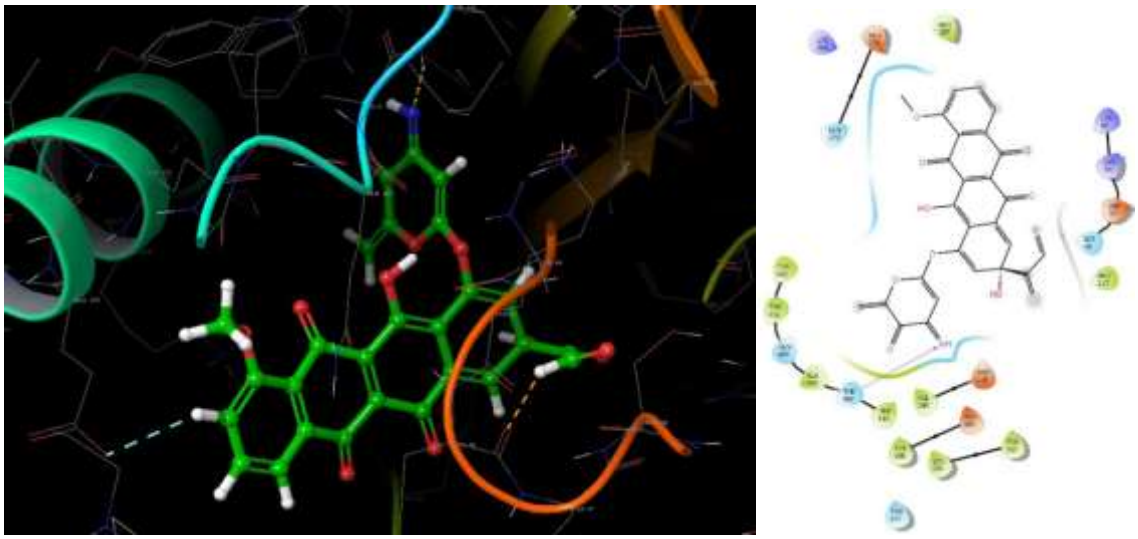

Fig. 10. Doxorubicin docked in cavity 1 with a docking score of -7.87 (left), the interaction diagram of doxorubicin ligand indicating the salt bridges between ligand and residue as Thr 409.

The molecular docking is based on algorithms and scoring functions, however inhibition concentration is calculated according to the results obtained from wet-lab experiments, so it is not possible to get an exact correlation between docking score and inhibitory activity. Docking gives the value with which the ligand binds to the protein and IC_{50} gives the value responsible for

inhibition. Therefore, docking scores cannot predict if the binding ligand is inhibiting enzyme function.

QA is an organic acid and involved in various fundamental pathways in plant metabolism and catabolism as intermediate or end products. It is an intermediate of the biochemically important "shikimate pathway" (Pereira et al., 2013). It is also one of the precursors of aromatic compounds in plants and micro-organisms. QA is a building block for the synthesis of several valuable secondary compounds, including coumaroyl and caffeoylquinic acid derivatives with significant biological activity in several drug-target areas (Cheynier et al., 2012). No previous reports were found on its HIV RT activity

4. Conclusions

Despite several efforts to develop inhibitory substances against the enzymes essential for proliferation of HIV, either synthetically or from medicinal plants, the development of a cure for HIV has still not been achieved. Metabolomic investigations can lead to a faster identification of molecules responsible for the observed bioactivity and could become a key component in the synthetic as well as natural biological approach to drug discovery. Knowledge of the 3D structure of ligand-protein complexes provides a valuable understanding of the function of molecular systems and plays a key-role in drug discovery. The main objective in the analyzing of molecular docking is to obtain ligand-receptor complexes with optimized conformation that possess lower binding free energy (Dar and Mir, 2017).

The results of this study showed that the polar *H. mimetes* extract had anti-HIV-1 activity at 25 µg/mL and at 2.5 µg/mL (> 98%) and its percentage inhibition activity against RT was 55.93 (± 3.3) at 50 µg/mL. QA isolated from this species exhibited good inhibition against RT with an IC_{50}

value of 53.82 (± 4.2) µg/mL. The molecular docking investigation predicted the binding cavity site and its related energy with which the ligand QA can bind with the RT-protein and have similar docking scores and emodel values as the positive drug controls.

In this study, molecular docking was performed to explore the possible binding mode of HIV-1-RT with QA isolated from *H. mimetes* using Glide XP. This investigation gave a better understanding of its mechanism of action against the RT. The conclusion drawn from the docking analysis was that cavity 4 had the highest binding affinity with HIV-1-RT. The QA-RT complex showed good stability and good H-bonding. Although the obtained IC_{50} values of QA and doxorubicin in the anti-RT bioassay were comparable, their molecular mode of action in terms of their active sites was different. Doxorubicin was able to attach to the receptor on the surface of the RT enzyme of HIV-1, while QA could enter the cavities of the RT enzyme due to the size of the molecule. The present study will aid in the better understanding of the activity of QA against RT and also gives a better understanding on the mechanism of action of doxorubicin as positive drug control which has not been reported previously. This study is the first report on the isolation and identification of QA from *H. mimetes* and its anti-RT activity and docking investigation on RT.

Acknowledgements

The authors are grateful to the Buffelskloof Nature Reserve research manager, Mr John Burrows, and Mr Alexander Heunis of the Voortrekker Nature Reserve in Pretoria for giving permission to collect plants and providing us with the plant material. The SWISS-SA collaboration (SA-JRP14) and the financial contributions made by the University of Basel and the CSIR and to the University of Pretoria are acknowledged for their continued support. The National Research Foundation of South Africa (NRF) is thanked for financial assistance. Special thanks to Dr

Mamoalosi Selepe at Department of Chemistry, University of Pretoria for help with UPLC-MS/MS) analysis.

References

Albayrak, S., Aksoy, A., Sagdic, O., Hamzaoglu, E., 2010. Compositions, antioxidant and antimicrobial activities of *Helichrysum* (Asteraceae) species collected from Turkey. Food Chem. 119, 114–122.

Appendino, G., Ottino, M., Marquez, N., Bianchi, F., Giana, A., Ballero, M., Sterner, O., Fiebich, B.L., Munoz, E., 2007. Arzanol, an anti-inflammatory and anti-HIV-1 phloroglucinol α-pyrone from Helichrysum italicum ssp. microphyllum. J. Nat. Prod. 70, 608–612.

Boccard, J., Rutledge, D.N., 2013. A consensus orthogonal partial least squares discriminant analysis (OPLS-DA) strategy for multiblock Omics data fusion. Anal. Chim. Acta 769, 30–39.

Breitling, R., Ceniceros, A., Jankevics, A., Takano, E., 2013. Metabolomics for secondary metabolite research. Metabolites 3, 1076–1083.

Cameron, S.I., Smith, R.F., Kierstead, K.E., 2005. Linking medicinal/nutraceutical products research with commercialization. Pharm. Biol. 43, 425–433.

Cheynier, V., Sarni-Manchado, P., Quideau, S., 2012. Recent advances in polyphenol research. John Wiley & Sons.

Cohen, M.S., Hellmann, N., Levy, J.A., DeCock, K., Lange, J., 2008. The spread, treatment, and prevention of HIV-1: evolution of a global pandemic. J. Clin. Invest. 118, 1244–1254.

Cretu, G., Morlock, G., Raluca, A., Miron, A.C.N., 2013. A high-performance thin-layer

chromatographic method for chlorogenic acid and hyperoside determination from berry extracts. Rom. Biotechnol. Lett. 18, 8657.

Dar, A.M., Mir, S., 2017. Molecular docking: approaches, types, applications and basic challenges. J Anal Bioanal Tech 8, 2.

Filho, R.J., de Sousa Falcão, H., Maria Batista, L., Barbosa Filho, M., Regina Piuvezam, M., others, 2010. Effects of plant extracts on HIV-1 protease. Curr. HIV Res. 8, 531–544.

Fonteh, P.N., Keter, F.K., Meyer, D., Guzei, I.A., Darkwa, J., 2009. Tetra-chloro-(bis-(3, 5-dimethylpyrazolyl) methane) gold (III) chloride: An HIV-1 reverse transcriptase and protease inhibitor. J. Inorg. Biochem. 103, 190–194.

Friesner, R.A., Murphy, R.B., Repasky, M.P., Frye, L.L., Greenwood, J.R., Halgren, T.A., Sanschagrin, P.C., Mainz, D.T., 2006. Extra precision glide: Docking and scoring incorporating a model of hydrophobic enclosure for protein- ligand complexes. J. Med. Chem. 49, 6177–6196.

Halgren, T., 2007. New method for fast and accurate binding-site identification and analysis. Chem. Biol. Drug Des. 69, 146–148.

Halgren, T.A., 2009. Identifying and characterizing binding sites and assessing druggability. J. Chem. Inf. Model. 49, 377–389.

Halgren, T.A., Murphy, R.B., Friesner, R.A., Beard, H.S., Frye, L.L., Pollard, W.T., Banks, J.L., 2004. Glide: a new approach for rapid, accurate docking and scoring. 2. Enrichment factors in database screening. J. Med. Chem. 47, 1750–1759.

Harder, E., Damm, W., Maple, J., Wu, C., Reboul, M., Xiang, J.Y., Wang, L., Lupyan, D.,

Dahlgren, M.K., Knight, J.L., others, 2015. OPLS3: a force field providing broad coverage of drug-like small molecules and proteins. J. Chem. Theory Comput. 12, 281–296.

Heyman, H.M., Maharai, V., Meyer, J.J.M., 2013. Identification of anti-HIV compounds in *Helichrysum* species (Asteraceae) by means of NMR-based metabolomic guided fractionation. University of Pretoria (Ph.D. thesis).

Heyman, H.M., Maharaj, V., Meyer, J.J.M., 2009. Metabolomic comparison of selected *Helichrysum* species to predict their antiviral properties. University of Pretoria (Master dissertation).

Heyman, H.M., Senejoux, F., Seibert, I., Klimkait, T., Maharaj, V.J., Meyer, J.J.M., 2015. Identification of anti-HIV active dicaffeoylquinic-and tricaffeoylquinic acids in *Helichrysum populifolium* by NMR-based metabolomic guided fractionation. Fitoterapia 103, 155–164.

Hillard, O.M., 1983. Flora of Southern Africa, Asteraceae, Part 7 Inuleae Fascicle 2 Gnaphaliinae (First Part), Volume 33. ed. Botanical Research Institute, Department of Agriculture, Pretoria, South Africa.

Kapewangolo, P., Hussein, A.A., Meyer, D., 2013. Inhibition of HIV-1 enzymes, antioxidant and anti-inflammatory activities of *Plectranthus barbatus*. J. Ethnopharmacol. 149, 184–190.

Lall, N., Hussein, A.A., Meyer, J.J.M., 2006. Antiviral and antituberculous activity of *Helichrysum melanacme* constituents. Fitoterapia 77, 230–232.

Liu, N.Q., Cao, M., Frédérich, M., Choi, Y.H., Verpoorte, R., van der Kooy, F., 2010. Metabolomic investigation of the ethnopharmacological use of *Artemisia afra* with NMR spectroscopy and multivariate data analysis. J. Ethnopharmacol. 128, 230–235.

Lourens, A.C.U., Reddy, D., Ba\cser, K.H.C., Viljoen, A.M., Van Vuuren, S.F., 2004. In vitro biological activity and essential oil composition of four indigenous South African *Helichrysum* species. J. Ethnopharmacol. 95, 253–258.

Lourens, A.C.U., Van Vuuren, S.F., Viljoen, A.M., Davids, H., Van Heerden, F.R., 2011. Antimicrobial activity and in vitro cytotoxicity of selected South African *Helichrysum* species. South African J. Bot. 77, 229–235.

Lourens, A.C.U., Viljoen, A.M., Van Heerden, F.R., 2008. South African *Helichrysum* species: a review of the traditional uses, biological activity and phytochemistry. J. Ethnopharmacol. 119, 630–652.

Meng, E.C., Pettersen, E.F., Couch, G.S., Huang, C.C., Ferrin, T.E., 2006. Tools for integrated sequence-structure analysis with UCSF Chimera. BMC Bioinformatics 7, 339.

Meyer, J.J.M., Afolayan, A.J., Taylor, M.B., Engelbrecht, L., 1996. Inhibition of herpes simplex virus type 1 by aqueous extracts from shoots of *Helichrysum aureonitens* (Asteraceae). J. Ethnopharmacol. 52, 41–43.

Meyer, J.J.M., Afolayan, A.J., Taylor, M.B., Erasmus, D., 1997. Antiviral activity of galangin isolated from the aerial parts of *Helichrysum aureonitens*. J. Ethnopharmacol. 56, 165–169.

Min, B.-S., Nakamura, N., Miyashiro, H., Kim, Y.-H., Hattori, M., 2000. Inhibition of human immunodeficiency virus type 1 reverse transcriptase and ribonuclease H activites by constituents of *Juglans mandshurica*. Chem. Pharm. Bull. 48, 194–200.

Mukhtar, M., Arshad, M., Ahmad, M., Pomerantz, R.J., Wigdahl, B., Parveen, Z., 2008. Antiviral potentials of medicinal plants. Virus Res. 131, 111–120.

Okada, T., Mochamad Afendi, F., Altaf-Ul-Amin, M., Takahashi, H., Nakamura, K., Kanaya, S., 2010. Metabolomics of medicinal plants: the importance of multivariate analysis of analytical chemistry data. Curr. Comput. Aided. Drug Des. 6, 179–196.

Pereira, C., Barros, L., Carvalho, A.M., Ferreira, I.C.F.R., 2013. Use of UFLC-PDA for the analysis of organic acids in thirty-five species of food and medicinal plants. Food Anal. Methods 6, 1337–1344.

Priya, R., Sumitha, R., Doss, C.G.P., Rajasekaran, C., Babu, S., Seenivasan, R., Siva, R., 2015. Molecular docking and molecular dynamics to identify a novel human immunodeficiency virus inhibitor from alkaloids of *Toddalia asiatica*. Pharmacogn. Mag. 11, S414.

Ramirez, D., 2016. Computational methods applied to rational drug design. Open Med. Chem. J. 10, 7.

Schauer, N., Fernie, A.R., 2006. Plant metabolomics: towards biological function and mechanism. Trends Plant Sci. 11, 508–516.

Schripsema, J., 2010. Application of NMR in plant metabolomics: techniques, problems and prospects. Phytochem. Anal. An Int. J. Plant Chem. Biochem. Tech. 21, 14–21.

Scott, G., Hewett, M.L., 2008. Pioneers in ethnopharmacology: the Dutch East India Company (VOC) at the Cape from 1650 to 1800. J. Ethnopharmacol. 115, 339–360.

Vidal, V., Potterat, O., Louvel, S., Hamy, F., Mojarrab, M., Sanglier, J.-J., Klimkait, T., Hamburger, M., 2012. Library-based discovery and characterization of daphnane diterpenes as potent and selective HIV inhibitors in Daphne gnidium. J. Nat. Prod. 75, 414–419.